Some Properties and Molecular Orbitals of Planar Heterodinuclear Phthalocyanines

Nagao Kobayashi*[a] and Hiroshi Ogata[a]

Keywords: Circular dichroism / Cyclic voltammetry / Phthalocyanines / UV/Vis spectroscopy

The electronic absorption and magnetic circular dichroism (MCD) spectra, and differential pulse (DP) voltammograms of planar heterodinuclear phthalocyanine (Pc) dimers consisting of Pc and pyrazinoporphyrazine (PyZ), [Mt_2PcPyZ (Mt = H_2 and Zn)] and of Pc and naphthalocyanine (Nc), [Mt_2PcNc (Mt = H_2 and Co)] have been recorded. These dimers commonly show broad absorption bands between ca. 500 and 1000 nm, while the DP voltammograms suggest that the dimers are unstable towards oxidation, and that the two relatively independent chromophore units interact with one another. Molecular orbital (MO) calculations using the ZINDO/S Hamiltonian were performed in order to enhance the interpretation of the experimental results. Dimer orbitals were expressed by coupling the orbitals of the same symmetry, of the constituting mononucleates. It was suggested that for the HOMO of the dimers, the contribution of the more electron-rich moiety is large, while conversely for the LUMO, the contribution of the more electron-deficient moiety is large. The calculations suggested that there are three prominent transitions in the Q band region of the heterodimers. The intensity and position of these bands were suggested to be affected by the constituting mononucleates.

Introduction

For three quarters of a century, mononuclear phthalocyanines (Pcs) have been the subject of an intensive study in both the academic and applied fields.[1] Cofacial sandwich type Pc dimers have been known since1936,[2] while the first planar dimer was reported in 1987.[3] Since then, many papers have been published on both cofacial Pc dimers[4] and planar homodimers of Pc and Pc derivatives.[5] However, reports on heterodinuclear planar dimers are still rare.[6] In particular, the physicochemical and electrochemical properties have not been well elucidated.[7] We report here on some spectroscopic and electrochemical properties, together with the results of molecular orbital (MO) calculations on planar heterodinuclear phthalocyanine-pyrazinoporphyrazine (Pc-PyZ) and phthalocyanine-naphthalocyanine (Pc-Nc) complexes, which were not described in our preliminary communications (Figure 1).[6a,6b,6d]

Results and Discussion

(i) Electronic Absorption and MCD Spectra

In the cases of H_4PcPyZ and H_4PcNc, there is an ambiguity as to the position of the pyrrole protons, thus it is not appropriate to compare their spectra with the results of the MO calculations. Figure 2 therefore shows the absorption and MCD spectra of PcPyZ and PcNc obtained by the addition of $(Bu)_4NOH$, and of Co_2PcNc. All compounds show broad Q bands which stretch from ca. 500 to 1000 nm, and which are not a simple superimposition from those of the constituting mononuclear *tert*-butylated Pc and PyZ or Nc. The Q bands of PcPyZ and PcNc are similar in shape, having at least two peaks, of which those at the shorter wavelength are broader. The Q bands of PcNc and Co_2PcNc appeared at almost the same wavelength, which is longer than that of PcPyZ by ca. 10 nm. The absorption coefficients of the two Q peaks of PcNc are larger than those of PcPyZ, consistent with the results of MO calculations described later.

The Q band MCD spectra of the three complexes have common characteristics. Negative Faraday *B*-terms appeared corresponding to the absorption peaks at a longer wavelength,[5m] and dispersion type, Faraday *A*-term like curves were observed, associated with the Q band peak at a shorter wavelength. In these molecules, there is no degeneracy in the excited states so that the Faraday *B*-terms are expected, theoretically, to be associated with each absorption peak. Considering that the tendency towards cofacial aggregation is much more significant for larger Ncs than Pcs,[11] that the cofacial aggregation produces a broad Q absorption band as seen at ca. 600−750 nm in Figure 2, and that the Q band MCD of cofacial Pc analogues does not reflect the molecular symmetry of the constituting molecules,[12] the dispersion type Faraday *A*-term like MCD signal corresponding to the Q absorption band at shorter wavelength may imply that the species in Figure 2 contains

[a] Department of Chemistry, Graduate School of Science, Tohoku University,
Sendai 980-8578, Japan
Fax: (internat.) + 81-22-217-7719
E-mail: nagaok@mail.tains.tohoku.ac.jp

  DOI: 10.1002/ejic.200300536

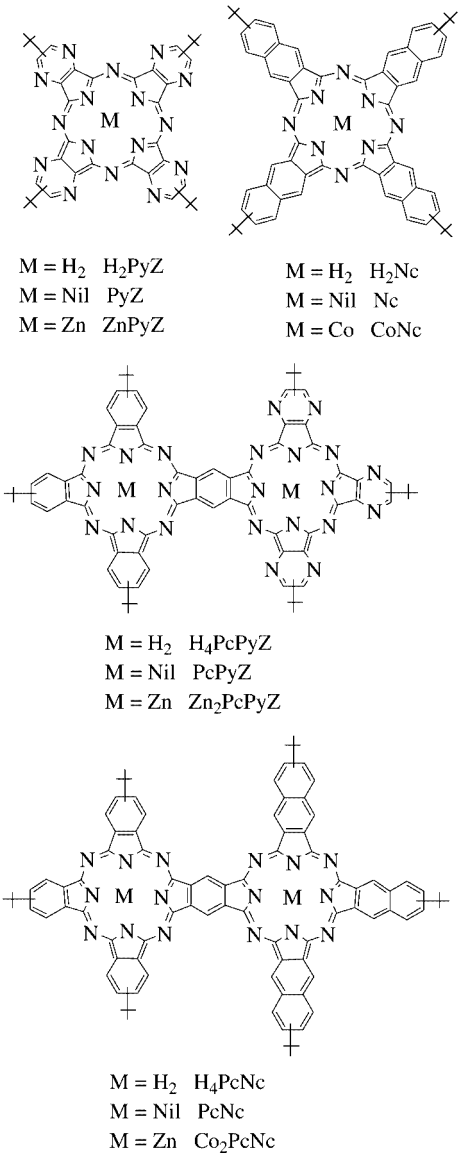

Figure 1. Structures and abbreviations of the compounds in this study

a certain amount of cofacially aggregated species. However, from our previous data[5m] in which the two Q_{00} bands of the homodinuclear planar Pc lie ca.1600−1800 cm^{-1} apart, together with the results of MO calculations on the compounds in the present study which will be discussed below, it is not unreasonable to expect the second Q_{00} band to appear at ca. 640−690 nm, since the other Q_{00} band lies at ca. 800−850 nm. Positive envelopes of the Faraday *B*-term superimposed with the pseudo Faraday *A*-terms at ca. 630−680 nm support this speculation. Another possibility for the interpretation of the dispersion type MCD curves at around 650−720 nm is that these are produced by two closely lying transitions, since MO calculations indicate two transitions in this region, differing from the case of the homodinuclear planar species [see section (iii)].

The apparent absorption coefficient of the B band of the Pc analogues is generally much smaller than that of the Q

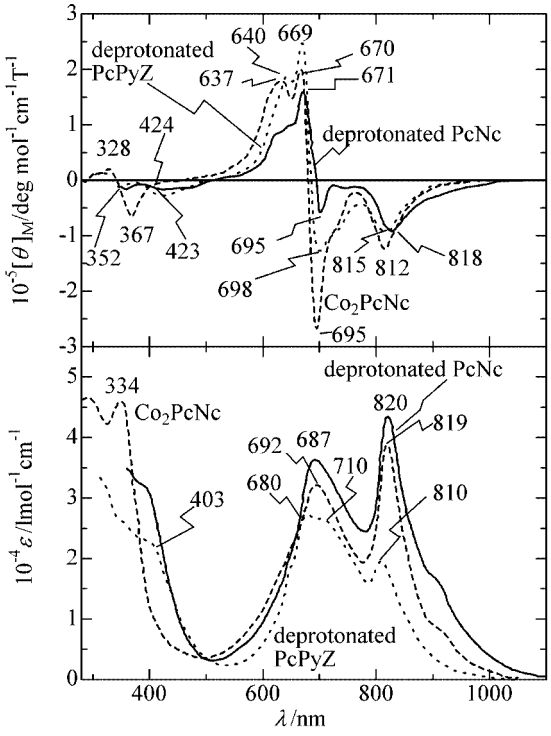

Figure 2. Electronic absorption (bottom) and MCD spectra (top) of (pyrrole proton-deprotonated) PcNc (solid lines), PcPyZ (dotted lines), and Co_2PcNc (broken lines)

band. Although we cannot directly compare the B band spectra of Zn_2PcPyZ and Co_2PcNc, since the central metal is different, the B bands of H_4PcPyZ and H_4PcNc appeared at 337 and 341 nm, and their relative intensity to the Q band is larger than in the monomeric species. When tetraammonium hydroxide was added to these metal-free species to form pyrrole-proton-deprotonated PcPyZ and PcNc, the intensity of the B band decreased and a shoulder appeared at ca. 400 nm for both compounds.

The MCD spectra show that the B band retains the characteristics of the Pc derivatives. Both H_4PcPyZ and H_4PcNc showed a dispersion type, pseudo Faraday *A*-term with a trough and peak at 372 and 320−321 nm, while their intensity was much smaller than that of the Q band, reflecting small angular momentum properties. In PcPyZ and PcNc, two weak pseudo Faraday *A*-terms appeared at around 403 and 366 nm, suggesting that many transitions are included in this region.

(ii) Voltammetry

Figure 3 shows differential pulse voltammograms of Zn_2PcPyZ, Co_2PcNc, and their constituting monomers in *o*-DCB. Unfortunately, we could not unify the type of central metal, since the compound which may be expressed as Co_2PcPyZ fragmented into the PyZ moiety in the cobalt insertion process, while the compound which is described as Zn_2PcNc fragmented during purification by column chromatography. The tetra-*tert*-butylated ZnPc showed two oxidation and reduction couples at 1.01, 0.21, −1.41, and −1.81 V, while ZnPyZ displayed the first oxidation poten-

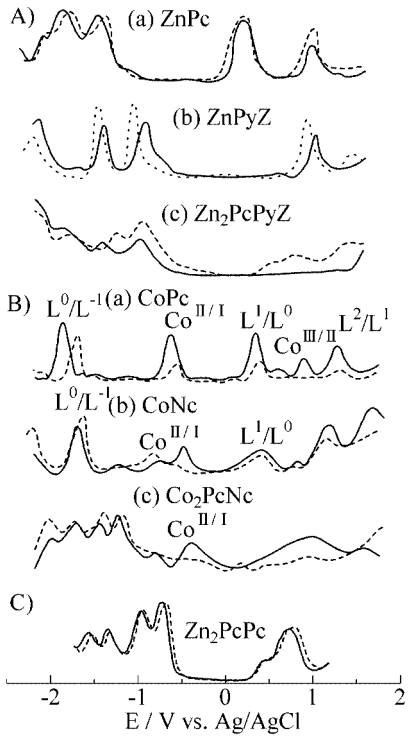

Figure 3. Differential pulse voltammograms of A) (a) ZnPc, (b) ZnPyZ, and (c) Zn_2PcPyZ, B) (a) CoPc, (b) CoNc, and (c) Co_2PcNc, and C) Zn_2PcPc (redrawn from ref.[5f]) in *o*-DCB containing 0.1 M TBAP. The sweep rate was 0.5 mV/s. The solid and broken lines are anodic and cathodic scans, respectively. L^0/L^{-1} and L^1/L^0 are the first reduction and oxidation of the ligand, respectively

tial at 1.03 V and three reduction couples at −0.97, −1.38, and −2.14 V due to the four electron-withdrawing pyrazine rings on the periphery. Zn_2PcPyZ, on the other hand, showed couples at ca. 1.36, 0.76, 0.50, −0.96, −1.34, −1.82, and ca. −2.2 V. Although the voltammograms are not clear, because of the instability of the compound in the positive potential region of the anodic scan, some of the other behavior (amount of current and splitting pattern) is similar to that of homodinuclear planar Pc dimers (voltammograms in C).[5f] That is, it appears as if the couples at 0.76 and 0.50 V correspond to the first oxidation, while those at −0.96 and −1.34, and −1.82 and −2.2 V correspond, respectively, to the first and second reductions of mononuclear species, suggesting that the voltammograms of Zn_2PcPyZ are caused by the interacting dipoles in the Pc and PyZ moieties.

The voltammograms of cobalt Pc derivatives differ from those of, for example, zinc, nickel, and copper derivatives in that they show couples due to the central metal, in addition to those of the ligand. On the basis of previous studies on cobalt Pcs,[13] the redox couples of *tert*-butylated CoPc and CoNc in this figure can be assigned as shown in the voltammograms. The voltammogram of Co_2PcNc is not as clear as that of the mononuclear species because of its low stability and small diffusion coefficient. However, four ligand redox couples characteristic of these types of compounds are explicitly seen at −1.22, −1.43, −1.73, and ca. −2.0 V, in addition to the $Co^{II/I}$ couple(s) which appeared at −0.36 (and −0.80) V, although the positive potential region is more irreversible and more ill-defined. Thus, the four ligand reduction redox couples strongly suggest that the dipoles in the CoPc and CoNc moieties are interacting without significant conjugation through the common benzene ring.

(iii) Molecular Orbital Calculations

In order to enhance our interpretation of the above spectroscopic and electrochemical properties, molecular orbitals (MOs) were calculated using the ZINDO/S Hamiltonian in the HyperChem. R5.1 program,[8] together with those of the constituting mononuclear molecules. The calculated electronic absorption spectra are shown in Figure 4 (all spectra were calculated for the zinc complexes, since Co^{II} in Pc, Nc, and PyZ is paramagnetic), with transition energies, oscillator strengths (*f*), and configurations summarized in Table 1. As detailed in previous publications,[14] in a one-electron description, the Q band of Pc analogues corresponds to a transition from the HOMO to the doubly degenerate LUMO. The B band is associated mainly with a transition from the HOMO-1 to the LUMO at the PPP level of calculations, while this is not clear at the ZINDO/S level of calculation since the B band is actually composed of two bands termed B1 and B2, and there is mixing of many configurations.[14f] For ZnPyZ and ZnPc, the present ZINDO/S calculations indicate the HOMO−LUMO transition and two prominent transitions in the B band region to be at 688 and 307/300 nm, and 699 and 292/278 nm, respectively, which is in approximate agreement with the experimental result (341 and 628 nm for ZnPyZ, and 349 and 671 nm for ZnPc in THF).[6a] This demonstrates the reliability of the calculations. As shown, in the case of mononuclear molecules, the Q band shifts to a longer wavelength in the order ZnPyZ, ZnPc, and ZnNc, with a con-

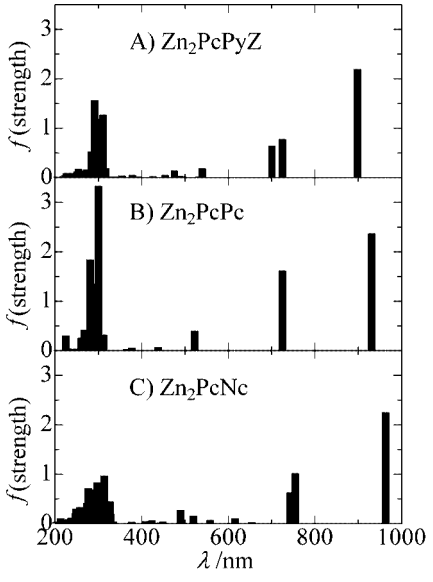

Figure 4. Calculated absorption spectra for A) Zn_2PcPyZ, B) Zn_2PcPc, and C) Zn_2PcNc

Table 1. Calculated transition energies, oscillator strengths (*f*), and configurations

Energy [nm]	*f*	Configurations[a]
ZnPyZ		
688	0.80	93→94 (88%)
688	0.80	93→95 (88%)
307	1.65	91→94 (51%) 92→94 (34%)
307	1.65	91→95 (51%) 92→95 (34%)
300	1.04	92→94 (54%) 91→94 (36%)
300	1.04	92→95 (54%) 91→95 (36%)
278	0.15	93→102 (59%) 88→94 (25%)
278	0.15	93→103 (59%) 88→95 (25%)
254	0.11	88→94 (62%) 93→102 (15%)
254	0.11	88→95 (62%) 93→103 (15%)
Zn_2PcPyZ		
898	2.19	171→172 (88%)
725	0.78	171→173 (51%) 171→174 (24%) 170→173 (10%)
701	0.64	171→174 (43%) 171→173 (29%) 170→173 (18%)
539	0.19	170→173 (47%) 170→174 (21%) 171→174 (19%)
475	0.14	171→178 (42%) 170→178 (30%) 170→174 (17%)
318	0.19	166→172 (36%) 168→172 (32%) 169→172 (18%)
311	1.27	169→173 (33%) 168→174 (15%) 169→174 (12%) 167→173 (11%)
304	1.20	167→174 (15%) 169→173 (14%)
302	0.42	165→173 (29%) 165→174 (18%) 169→172 (14%) 169→175 (11%)
299	0.68	170→181 (25%) 168→173 (18%) 169→173 (13%)
298	0.95	163→172 (24%) 167→172 (16%)
298	0.32	164→173 (24%) 164→174 (23%) 163→172 (14%)
294	0.30	166→174 (17%) 164→172 (16%)
294	0.13	166→173 (17%)
291	1.57	167→172 (15%) 166→172 (12%) 165→173 (11%) 167→175 (11%)
287	0.22	171→186 (21%) 163→172 (12%)
283	0.53	171→189 (32%) 170→189 (14%)
282	0.15	171→186 (22%) 166→175 (11%) 170→187 (10%)
278	0.15	171→191 (37%) 171→189 (13%)
274	0.17	160→172 (25%)
269	0.14	171→190 (16%) 171→188 (12%) 161→173 (11%)
254	0.17	162→173 (25%) 159→172 (14%) 162→174 (12%) 158→172 (11%)
251	0.12	159→173 (20%) 162→172 (17%) 159→174 (12%)
ZnPc		
699	1.06	93→94 (87%)
699	1.06	93→95 (87%)
292	1.18	93→102 (36%) 92→94 (28%) 91→94 (13%) 91→95 (11%)
292	1.18	93→103 (36%) 92→95 (28%) 91→95 (13%) 91→94 (11%)
287	0.48	91→94 (53%) 93→102 (14%) 85→95 (11%)
287	0.48	91→95 (53%) 93→103 (14%) 85→94 (11%)
278	1.06	92→94 (50%) 93→102 (34%)
278	1.06	92→95 (50%) 93→103 (34%)
Zn_2PcNc		
964	2.25	198→199 (77%)
755	1.02	198→200 (59%) 197→200 (34%)
744	0.63	198→201 (81%)
616	0.11	197→199 (46%) 198→202 (33%) 198→199 (15%)
519	0.16	197→201 (64%) 198→203 (12%)
490	0.27	198→203 (34%) 197→203 (24%) 197→201 (21%)
328	0.20	195→199 (34%) 197→205 (24%) 198→205 (14%) 192→199 (11%)
326	0.44	196→199 (39%) 195→200 (21%) 194→199 (11%)
317	0.28	193→199 (28%) 196→199 (20%) 194→199 (14%)
315	0.13	198→210 (55%) 197→210 (33%)
313	0.97	196→200 (42%) 192→199 (30%)
298	0.19	195→200 (18%) 185→199 (18%) 196→199 (15%)
297	0.83	192→199 (19%) 198→219 (13%) 194→200 (12%)
295	0.44	194→202 (18%) 198→218 (14%) 193→199 (11%) 194→199 (11%) 193→202 (11%) 198→220 (10%)
295	0.15	187→199 (16%) 189→200 (14%) 195→199 (10%)
293	0.47	189→199 (42%) 187→200 (20%)
293	0.16	198→219 (32%) 193→201 (14%) 191→201 (13%)
292	0.62	190→201 (50%) 188→201 (17%)
288	0.50	195→200 (17%) 185→199 (16%) 192→200 (16%)
281	0.69	189→200 (26%) 187→199 (13%) 194→201 (13%) 195→199 (11%)

Table 1. *(Continued)*

Energy [nm]	*f*	Configurations[a]
279	0.21	197→209 (32%) 1972→07 (11%)
277	0.72	198→222 (18%) 197→209 (13%) 191→199 (12%)
274	0.42	192→200 (44%) 185→199 (20%)
270	0.32	187→200 (43%) 189→199 (12%)
269	0.12	193→201 (24%) 198→221 (20%) 194→201 (10%)
261	0.10	187→199 (23%) 197→212 (20%)
258	0.33	185→200 (31%) 186→201 (18%)
249	0.13	183→202 (18%) 183→199 (14%) 186→199 (12%)
249	0.18	192→200 (14%) 192→203 (14%) 195→203 (11%) 186→199 (11%)
ZnNc		
771	1.34	129→130 (95%)
771	1.34	129→131 (95%)
324	0.54	129→138 (54%)
324	0.54	129→139 (54%)
316	0.26	128→130 (77%) 129→139 (10%)
316	0.26	128→131 (77%) 129→138 (10%)
285	2.09	124→131 (36%) 123→130 (18%) 124→130 (12%) 125→130 (11%)
285	2.09	124→130 (36%) 123→131 (18%) 124→131 (12%) 125→131 (11%)
246	0.12	120→130 (60%)
246	0.12	120→131 (60%)
242	0.77	128→134 (24%) 125→130 (20%) 127→133 (14%) 126→132 (11%)
242	0.77	128→135 (24%) 125→131 (20%) 126→133 (14%) 127→132 (11%)
Zn_2PcPc		
931	2.37	171→172 (89%)
726	1.62	171→173 (83%) 170→174 (10%)
522	0.40	170→174 (82%) 171→173 (12%)
312	0.32	167→172 (47%) 169→172 (43%)
309	0.14	170→178 (56%) 171→176 (15%) 170→184 (13%)
300	3.33	169→173 (60%) 168→174 (11%)
296	0.65	164→172 (46%) 165→175 (%)
294	0.12	166→173 (40%) 163→174 (40%)
290	1.35	171→188 (24%) 170→186 (16%) 164→172 (10%)
287	0.45	171→185 (44%) 170→187 (16%)
287	0.68	170→179 (40%) 171→180 (10%) 170→190 (10%)
280	1.84	169→172 (26%) 171→188 (25%) 167→172 (18%) 168→175 (11%)
267	0.42	160→173 (15%) 167→173 (14%) 161→174 (14%) 164→173 (12%)
260	0.26	155→172 (22%) 158→173 (20%) 162→173 (16%)

[a] Excited states with energy less than ca. 3.9 eV and *f* greater than 0.10 are shown.

comitant increase in the absorption coefficient, as has been substantiated by experiments[15] and reproduced by MO calculations[16] using the PPP method.[17] The purity of the Q band also increases in this order, since the configurations of the HOMO−LUMO transition increases.

Turning to the heterodinuclear Pc analogues in this study, the pair of orbitals comprising the lowest unoccupied level in a mononuclear unit split into two levels (Figure 5), so that two split Q bands are calculated at a longer wavelength: 898 and 725 for Zn_2PcPyZ and 964 and 755 nm for Zn_2PcNc (under the same conditions, the Q bands of the homodinuclear Zn_2PcPc were predicted at 931 and 726 nm). The calculated values lie in the correct direction, but fall towards somewhat longer wavelengths compared with the experimental values. In addition, the values indicate that the Q band position depends on that of the constituting units of the dimer. That is, the two Q bands estimated for Zn_2PcPyZ (898 and 725 nm) are at shorter wavelengths than those of Zn_2PcPc (931 and 726 nm), while those of Zn_2PcNc (964 and 755 nm) are calculated at even longer wavelengths. This, however, does not necessarily hold for the Q band intensity. The *f* values for the two Q bands for Zn_2PcPyZ, Zn_2PcPc, and Zn_2PcNc are 2.19 and 0.78, 2.37 and 1.62, and 2.25 and 1.02, respectively (the Q bands at longer wavelengths are always more intense), suggesting that the Q band of the homodimer may be stronger than that of the heterodimers. The values also suggest that in the heterodimers, the Q band of the dimers having larger π conjugation systems may be stronger. As shown by the configurations in Table 1, the calculations predict that for all the planar binucleates, in the one-electron description, the Q band to lower energy corresponds to a transition from the HOMO to LUMO, while that to higher energy is mainly associated with a transition from the HOMO to the LUMO+1. Of these, concerning configurations of the longer wavelength Q band, the contributions of the HOMO−LUMO transition for Zn_2PcPyZ, Zn_2PcPc, and Zn_2PcNc are 88, 89, and 77%, respectively, as for the above *f* values, suggesting that the contribution does not vary systematically with the structure of the constituting units.

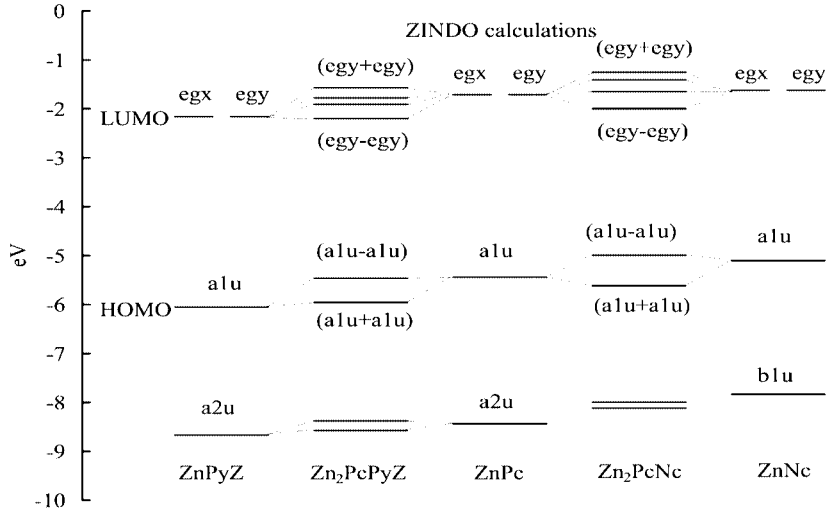

Figure 5. Partial molecular orbital energy diagram for Zn_2PcPyZ and Zn_2PcNc, and for ZnPyZ, ZnPc, and ZnNc, and their mutual relationships. The parentheses near each MO of the dimers indicate the expression of MO by the notation in D_{4h} symmetry, which is used for ZnPyZ, ZnPc, and ZnNc

From the configurational values for the HOMO to LUMO transition (Table 1), the purity of the transition at the longest wavelength of the dimers is similar to that of constituting monomers (88, 87, and 95% for ZnPyZ, ZnPc, and ZnNc, respectively) except for Zn_2PcNc.

Another notable point for the heterodimer spectra is the presence of a third transition lying closely in energy to the second transition (701 nm for Zn_2PcPyZ and 744 nm for Zn_2PcNc). This fairly intense band is ascribed mainly to the HOMO to LUMO+2 transition. It is possible, therefore, to consider that because of this transition, the experimental Q band at a shorter wavelength is much broader than that at a longer wavelength, since two closely lying transitions can produce a broad band due to superimposition. If this is the case, the dispersion type MCD associated with the second Q absorption peak can be considered to be produced by closely lying Faraday *B*-terms of opposite signs.

MO numbers 93, 171, 93, 198, and 129 are the HOMOs for ZnPyZ, Zn_2PcPyZ, ZnPc, Zn_2PcNc, and ZnNc, respectively. The data for the homodinuclear Zn_2PcPc are also shown for comparative purposes.

In the B band region, the calculated data of the constituting compounds are not complicated, particularly for ZnPyZ, although those of ZnNc are more complex because of the involvement of the transitions localized in the naphthalene ring. In contrast, the B band region of the dimers is very complex. The most intense region was predicted at 311 (f = 1.27) and 304 nm (f = 1.20) for Zn_2PcPyZ and 313 (f = 0.97) and 297 nm (f = 0.83) for Zn_2PcNc, implying that the more intense B band region of the two compounds would appear at a similar wavelength, if the two compounds could be prepared (we could not obtain Zn_2PcNc, since it fragmented during column chromatography).

Figure 5 shows how the four frontier orbitals in mononuclear constituting molecules split in the heterodimers. This figure indicates that two monomer orbitals having the same symmetry residing in different constituting units couple and produce two dimer orbitals, and that the extent of the splitting is larger for orbitals having a larger coefficient along the axis connecting the two constituting units (for the shape of orbitals, see Figure 6). That is, of the a_{1u} and a_{2u} orbitals, a_{1u} is larger, while of the e_{gx} and e_{gy} orbitals, the latter is larger. Furthermore, comparison of the orbital energies of the constituting monomers and the resulting dimers suggests that for the HOMO of the dimers the contribution of an electron-richer moiety is larger, while for the LUMO of the dimers the contribution of a more electron-deficient moiety is large. Indeed, if we compare the energy difference between the HOMO of Zn_2PcPyZ and those of ZnPc and ZnPyZ, the difference between Zn_2PcPyZ and ZnPc is much smaller than that between Zn_2PcPyZ and ZnPyZ. Similarly, the energy difference between the HOMO of Zn_2PcNc and ZnNc is much smaller than that between Zn_2PcNc and ZnPc. Accordingly, we can conclude that for the HOMO of Zn_2PcPyZ, the contribution of the Pc moiety is more significant than that of the PyZ moiety. In a similar manner, for the HOMO of Zn_2PcNc, the contribution of the Nc moiety is larger than that of the Pc moiety. In the case of the LUMO, the inverse relationship is observed for the energy difference between the LUMO of constituting monomers and the resultant dimers. Thus, the contribution of the PyZ moiety appears larger than that of the Pc moiety for the LUMO of Zn_2PcPyZ.

We can correlate the experimental redox potentials (Figure 3) with the calculated MO energies from Figure 5. Since relatively clear voltammetric curves were obtained in the negative potential region for all of the compounds, the reduction potentials of the two monomers and the resulting dimer complex can be discussed and compared with data in Figure 5. The first reduction in ZnPc and ZnPyZ corresponds to an addition of an electron to the e_g LUMO. A more negative potential (−1.41 V) is obtained for ZnPc

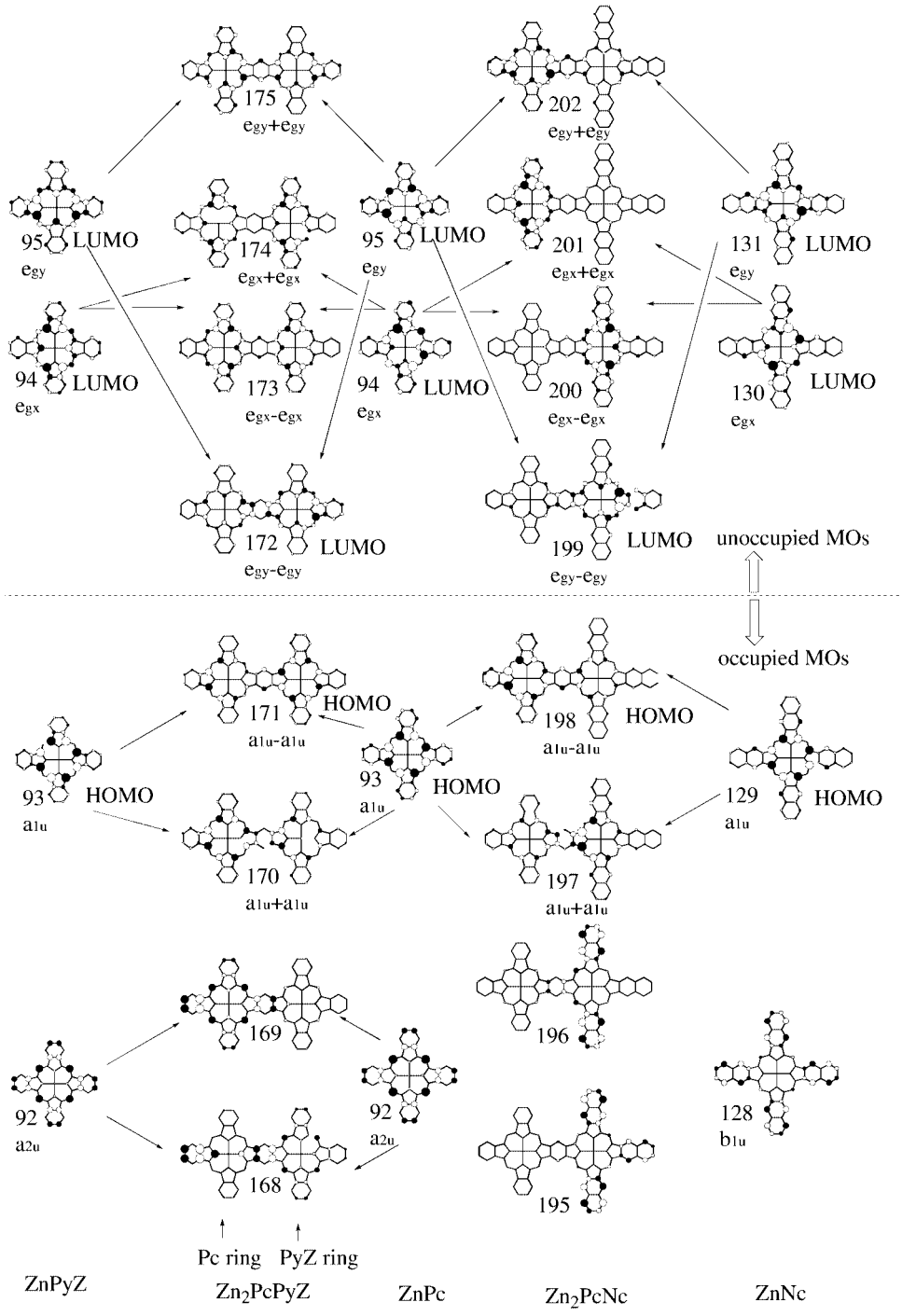

Figure 6. Eight frontier orbitals of Zn_2PcPyZ and Zn_2PcNc and four frontier orbitals of ZnPyZ, ZnPc, and ZnNc. The parentheses under each MO of the dimers indicate the expression of MO by the notation in D_{4h} symmetry, which is used for ZnPyZ, ZnPc, and ZnNc

than (−0.97 V) for ZnPyZ (Figure 3), as a result of the lower electron-density of ZnPyZ due to the electron-withdrawing property of the four peripheral pyrazine rings. Since the e_g orbital of ZnPc sits at a higher energy than that of ZnPyZ (Figure 5), the reduction of ZnPc is expected to require a higher potential. When ZnPc and ZnPyZ are laterally fused to form Zn_2PcPyZ, the calculated LUMO energy is very similar to that of ZnPyZ (Figure 5). As expected, the first reduction potentials of ZnPyZ and Zn_2PcPyZ are found to be very close [Figure 3, curves (b) and (c)]. The calculated LUMO energies of ZnPc and ZnNc are almost identical. The first reduction potentials of these compounds are therefore expected to be very similar. The LUMO energy of the resulting Zn_2PcNc dimer drops substantially, relative to that of ZnPc. As a result, the first reduction step for the Mt_2PcNc dimer occurs at a less negative potential than that of the corresponding MtPc or MtNc monomers. This feature is observed experimentally in the voltammograms of cobalt complexes in Figure 3 (curves in B). There is therefore clearly a close agreement

between the calculated LUMO energies and the experimental reduction potentials. The HOMO energies and the oxidation potentials could not be compared in a similar manner, however, since the voltammograms are ill-defined in the positive potential region.

Figure 6 displays the four frontier orbitals of each mononuclear molecule and eight frontier orbitals of the resulting heterodimers. This figure clearly shows that the dimer orbitals are composed of the monomer orbitals with the same symmetry, since the dimer orbitals can be expressed as linear combinations of monomer orbitals of the same symmetry (see the notation below each MO). In addition, supporting the conclusions in Figure 5, for the HOMO of the dimer, the coefficient of the electron-richer moiety is large (i.e. in Zn_2PcPyZ, the coefficients in the Pc moiety are larger than those in the PyZ moiety, and similarly in Zn_2PcNc the coefficients in Nc are larger than those in the Pc moiety). Conversely, in the case of the LUMO, the coefficients in the more electron-deficient moiety is large (the PyZ moiety in Zn_2PcPyZ, and the Pc moiety in Zn_2PcNc).

Conclusion

The electronic absorption and magnetic circular dichroism (MCD) spectra, and differential pulse (DP) voltammograms of planar heterodinuclear phthalocyanine (Pc) dimers consisting of Pc and pyrazinoporphyrazine (PyZ) [Mt_2PcPyZ (Mt = H_2 and Zn)] and Pc and naphthalocyanine (Nc) [Mt_2PcNc (Mt = H_2 and Co)] have been recorded, and their properties interpreted by MO calculations using the ZINDO/S Hamiltonian. These dimers commonly show broad absorption bands between ca. 500 and 1000 nm, while the DP voltammograms suggest that the dimers are unstable to oxidation, and that, in these compounds, two relatively independent chromophore units interact. Dimer orbitals were found to be expressed by linear combinations of the orbitals of the constituting mononuclear orbitals of the same symmetry. It was suggested that for the HOMO of the dimers, the contribution of the electron-richer moiety is large, while, conversely, for the LUMO the contribution of the more electron-deficient moiety is large. The heterodimers showed two intense Q bands experimentally. Our calculations suggested that the position and intensity of these bands were affected by those of the constituting mononucleates. That is, PcPyZ dimers have a split Q band at shorter wavelengths than those of PcNc dimers. Of the two heterodimers, the Q band intensity of the PcNc dimer, i.e. the dimer consisting of larger π conjugation systems, appears larger than that of the PcPyZ dimer, since the calculated Q band of PyZ appears at a shorter wavelength and is weaker than that of Nc.

Experimental Section

(i) Measurements: Mass spectra were obtained with a JEOL JMS-HX110 mass spectrometer using *m*-nitrobenzyl alcohol (NBA) as a matrix (FAB mass). Electronic absorption spectra were recorded with a Hitachi U-3410 spectrophotometer using THF as a solvent. Magnetic circular dichroism (MCD) measurements were made with a JASCO J-725 spectrophotometer equipped with a JASCO electromagnet that produces magnetic fields of up to 1.09 T. Its magnitude was expressed in terms of molar ellipticity per tesla, $[\theta]_M$ (in $deg \cdot mol^{-1} \cdot dm^3 \cdot cm^{-1} \cdot T^{-1}$). The 400 MHz ^{1}H NMR spectral measurements were made with a JEOL-GSX-400 instrument. IR spectra were run on a Shimadzu FTIR-8100M spectrometer using KBr discs. Differential pulse voltammetry (DPV) experiments were carried out with conventional three-electrode cells, in which a platinum wire auxiliary electrode, a glassy carbon working electrode (0.07 cm^2), and an Ag/AgCl wire reference electrode were employed. The solvent for the electrochemical measurements, *o*-dichlorobenzene (*o*-DCB, Nacalai Tesque, specially prepared for HPLC) was used as supplied. Tetrabutylammonium perchlorate (TBAP) was used as an electrolyte. All electrochemical work was carried out under an atmosphere of dry nitrogen. DPV data were recorded with a Yanaco P-1100 polarographic analyzer connected to a Watanabe WX 4401 *XY* recorder.

(ii) Computational Method: MO calculations were performed using HyperChem. software[8] within the ZINDO/S level, in which the overlap weighting factors for σ-σ and π-π were 1.267 and 0.585, respectively. For the configuration interaction (CI) calculations, all singly excited configurations of up to 8 eV were included.

(iii) Materials: Deprotonation of the pyrrole proton in dinuclear metal-free species was affected by adding a small amount of tetra-*n*-butylammonium hydroxide. Tetra-*tert*-butylphthalocyaninatocobalt, CoPc, and tetra-*tert*-butylnaphthalocyaninatocobalt, CoNc, were used as in our previous paper.[9]

Tetra-*tert*-butylpyrazinoporphyrazinatozinc (ZnPyZ): This compound was obtained by zinc insertion using $Zn(OAc)_2$ to metal-free tetra-*tert*-butylpyrazinoporphyrazine[10] in EtOH/1,2-dichloroethane (1:1 v/v), and purified using a basic alumina column and CH_2Cl_2/MeOH as eluent in 71% yield. ^{1}H NMR (400 MHz, $CDCl_3$, TMS, ppm): δ = 9.87−9.67 (s, 4 H, Ar-H), 2.13−1.93 (m, 36 H, *t*Bu). $C_{40}H_{40}N_{16}Zn \cdot 3H_2O$: calcd. C 55.59, H 5.36, N 25.93; found C 55.02, H 5.56, N 25.27.

Tetra-*tert*-butylphthalocyaninatozinc (ZnPc): This compound was also obtained by zinc insertion to metal-free tetra-*tert*-butylphthalocyanine[6b] in EtOH/1,2-dichloroethane (1:1 v/v) in the dark for 15 h, and subsequent purification using a basic alumina and CH_2Cl_2. $C_{48}H_{48}N_8Zn$: calcd. C 71.85, H 6.03, N 13.97; found C 71.23, H 6.50, N 13.34.

Hexa-*tert*-butylphthalocyaninylpyrazinoporphyrazinatodizinc (Zn_2PcPyZ): A mixture of metal-free hexa-*tert*-butylphthalocyaninylpyrazinoporphyrazine,[6a] H_4PcPyZ (5.0 mg, 0.0039 mmol) and $Zn(OAc)_2$ (17 mg, 0.077 mmol) were refluxed in 1,2-dichloroethane/ EtOH (1:1 v/v) in the dark for 15 h, and after evaporating the solvent, the residue was chromatographed over a basic alumina column using a mixture of CH_2Cl_2 and MeOH, to give 5.0 mg (90% yield) of the desired dizinc complex, Zn_2PcPyZ as a blue powder. ^{1}H NMR (400 MHz, $CDCl_3$, TMS, ppm): δ = 9.5−7.0 (br, 14 H, Ar-H), 2.1−1.7 (m, 54 H, *t*Bu). MS (FAB, NBA): *m*/*z*: 1419 [M]. $C_{76}H_{68}N_{22}Zn_2 \cdot 2H_2O$: calcd. C 62.68, H 4.98, N 21.16; found C 62.35, H 5.41, N 20.77.

Hexa-*tert*-butylphthalocyaninylnaphthalocyaninatodicobalt (Co_2PcNc): A mixture of metal-free hexa-*tert*-butylphthalocyaninylnaphthalocyanine[6b] (4.0 mg, 0.0028 mmol) and $CoCl_2$ (7.2 mg, 0.056 mmol) was refluxed in DMF (2.0 mL) for 30 min. After evap-

oration of the solvent, the residue was purified using a basic alumina column and CH_2Cl_2/MeOH as eluent, to give 3.8 mg (87.5% yield) of the desired Co_2PcNc as a blue powder. MS (FAB, NBA): *m/z*: 1550 [M]. $C_{94}H_{80}Co_2N_{16}{\cdot}H_2O$: calcd. C 71.93, H 5.27, N 14.28; found C 71.29, H 5.46, N 13.80.

Acknowledgments

This research was partially supported by the Ministry of Education, Science, Sports and Culture, a Grant-in-Aid for the COE project, Giant Molecules and Complex Systems, 2003.

[1] [1a] *Phthalocyanine. Properties and Applications* (Eds.: C. C. Leznoff, A. B. P. Lever), VCH Publications: New York. **1989, 1993, 1993, 1996**; Vols. I, II, III, and IV. [1b] *The Porphyrin Handbook* (Eds.: K. M. Kadish, K. M. Smith, R. Guilard), Academic Press: New York, **2003**, Vols. 15−20. [1c] *Phthalocyanine. Chemistry and Functions* (Eds.: H. Shirai, N. Kobayashi), IPC: Tokyo, **1997**. [1d] *The Phthalocyanines* (Eds.: F. H. Moser, A. H. Thomas), CRC Press, Boca Raton, FL, **1983**, Vols. 1 and 2.

[2] P. A. Barett, C. E. Dent, R. P. Linstead, *J. Chem. Soc.* **1936**, 1719−1736.

[3] C. C. Leznoff, H. Lam, S. M. Marcuccio, W. A. Nevin, P. Janda, N. Kobayashi, A. B. P. Lever, *J. Chem. Soc., Chem. Commun.* **1987**, 699−701.

[4] J. Jiang, K. Kasuga, D. P. Arnold, in: *Supramolecular Photosensitive and Electroactive Materials* (Ed.: H. S. Nalwa), Academic Press: New York, **2001**; Chapter 2, pp. 113−210.

[5] [5a] N. Kobayashi, M. Numao, R. Kondo, S. Nakajima, T. Osa, *Inorg. Chem.* **1991**, *30*, 2241−2244. [5b] N. Kobayashi, *J. Chem. Soc., Chem. Commun.* **1991**, 1203−1205. [5c] D. Lelievre, L. Bosio, J. Simon, J. J. Andre, F. Bensebaa, *J. Am. Chem. Soc.* **1992**, *114*, 4475−4479. [5d] D. Lelievre, O. Damette, J. Simon, *J. Chem. Soc., Chem. Commun.* **1993**, 939−940. [5e] J. Yang, M. R. Mark, *Tetrahedron Lett.* **1993**, *33*, 5223−5226. [5f] N. Kobayashi, H. Lam, W. A. Nevin, P. Janda, C. C. Leznoff, T. Koyama, A. Monden, H. Shirai, *J. Am. Chem. Soc.* **1994**, *116*, 879−890. [5g] T. F. Baumann, A. G. M. Barrett, B. M. Hoffman, *Inorg. Chem.* **1997**, *36*, 5661−5665. [5h] S. J. Lange, H. Nie, C. L. Stern, A. G. M. Barrett, B. M. Hoffman, *Inorg. Chem.* **1998**, *37*, 6435−6443. [5i] B. Hauschel, R. Jung, M. Hanack, *Eur. J. Inorg. Chem.* **1999**, 693−703. [5j] A. G. Montalban, W. Jarrel, E. Riguet, Q. J. McCubbin, M. E. Anderson, A. J. P. White, D. J. Williams, A. G. M. Barrett, B. M. Hoffman, *J. Org. Chem.* **2000**, *65*, 2472−2478. [5k] M. J. Cook, M. J. Heeney, *Chem. Eur. J.* **2000**, *6*, 3958−3967. [5l] E. M. Garcia-Frutos, F. Fernandez-Lazaro, E. M. Maya, P. Vazquez, T. Torres, *J. Org. Chem.* **2000**, *65*, 6841−6846. [5m] N. Kobayashi, T. Fukuda, D. Lelievre, *Inorg. Chem.* **2000**, *39*, 3632−3637. [5n] N. Kobayashi, A. Muranaka, V. N. Nemykin, *Tetrahedron. Lett.* **2001**, *42*, 913−915.

[6] [6a] N. Kobayashi, Y. Higashi, T. Osa, *J. Chem. Soc., Chem. Commun.* **1994**, 1785−1786. [6b] N. Kobayashi, Y. Higashi, T. Osa, *Chem. Lett.* **1994**, 1813−1816. [6c] G. Torre, M. V. Martinez-Diaz, P. R. Ashton, T. Torres, *J. Org. Chem.* **1998**, *63*, 8888−8893. [6d] K. Ishii, N. Kobayashi, Y. Higashi, T. Osa, D. Lelievre, J. Simon, S. Yamauchi, *Chem. Commun.* **1999**, 969−970.

[7] N. Kobayashi, *Coord. Chem. Rev.* **2002**, *227*, 129−152.

[8] *HyperChem. R5.1 Pro*, Hypercube Inc., Gainesville, FL, **1997**.

[9] N. Kobayashi, S. Nakajima, T. Osa, *Inorg. Chim. Acta* **1993**, *210*, 131−133.

[10] E. G. Gal'pern, E. A. Luk'yanets, *Acad. Nauk. SSSR. Bull. Chem. Sci.* **1973**, *22*, 1925.

[11] [11a] S. Tai, N. Hayashi, *J. Chem. Soc., Perkin Trans.2* **1991**, 1275−1279. [11b] S. Tai, N. Hayashi, M. Katayose, *Prog. Org. Coatings.* **1994**, *24*, 323−339.

[12] N. Kobayashi, M. Togashi, T. Osa, K. Ishii, S. Yamauchi, H. Hino, *J. Am. Chem. Soc.* **1996**, *118*, 1073−1085.

[13] [13a] W. A. Nevin, W. Liu, S. Greenberg, M. R. Hempstead, S. M. Marcuccio, M. Melnik, C. C. Leznoff, A. B. P. Lever, *Inorg. Chem.* **1987**, *26*, 891−899. [13b] N. Kobayashi, H. Lam, W. A. Nevin, P. Janda, C. C. Leznoff, A. B. P. Lever, *Inorg. Chem.* **1990**, *29*, 3415−3425.

[14] [14a] M. Gouterman, G. H. Wagniere, *J. Mol. Spectrosc.* **1963**, *11*, 108−127. [14b] B. W. Dale, *Trans. Faraday Soc.* **1969**, *65*, 331−339. [14c] A. Henriksson, B. Roos, M. Sundbom, *Theor. Chim. Acta* **1972**, *27*, 303−313. [14d] L. K. Lee, N. H. Sabelli, P. R. LeBreton, *J. Phys. Chem.* **1982**, *86*, 3926−3931. [14e] A. M. Schaffer, M. Gouterman, *Theor. Chim. Acta* **1972**, *25*, 62−82. [14f] J. Mack, M. J. Stillman, in: *The Porphyrin Handbook* (Eds.: K. M. Kadish, K. M. Smith, R. Guilard), Academic Press, New York, **2003**, Vols. 16, Chapter 103, pp. 43−116.

[15] E. A. Luk'yanets, *Electronic Spectra of Phthalocyanines and Related Compounds*, NIOPIK, Moscow, **1989**.

[16] [16a] S. Dong, B. Liu, J. Liu, N. Kobayashi, *J. Porphyrins Phthalocyanes.* **1997**, *1*, 333−340. [16b] N. Kobayashi, H. Konami, in: *Phthalocyanines-properties and Applications* (Eds.: C. C. Leznoff, A. B. P. Lever), VCH, New York, **1996**, Vol. 4, Chapter 9, pp. 343−404.

[17] [17a] R. Pariser, R. G. Parr, *J. Chem. Phys.* **1953**, *21*, 466−471, 767−776. [17b] J. A. Pople, *Trans. Faraday Soc.* **1953**, *49*, 1375−1385.

Received August 4, 2003
Early View Article
Published Online November 28, 2003